DASI: A Degree Angular Scale Interferometer for Imaging Anisotropy in the Cosmic Microwave Background

N. W. Halverson[a], J. E. Carlstrom, M. Dragovan, W. L. Holzapfel, and J. Kovac

Department of Astronomy and Astrophysics, University of Chicago, Chicago, IL 60637

ABSTRACT

The Degree Angular Scale Interferometer (DASI) is a compact cm-wave interferometer designed to image anisotropy in the Cosmic Microwave Background (CMB) and to measure its angular power spectrum. The power spectrum will be densely sampled over the ℓ range 160 to 710, corresponding to angular scales of 0.25 to 1.15 degrees. DASI consists of 13 elements. Each element consists of a 20-cm diameter lensed corrugated horn followed by a cooled low-noise HEMT amplifier operating from 26 - 36 GHz. All elements are mounted on a single alt-az mount, which fixes the projected baselines and obviates an IF tracking delay. The mount also includes rotation of the aperture plane along the line of sight to improve the u, v coverage and the control of instrumental systematics. The 10 GHz IF bandwidth will be correlated in 1 GHz bands to provide spectral index information. The instrument is scheduled to be completed in Summer 1998. After extensive testing it will be deployed at the South Pole for year-round operation starting in November 1999.

Keywords: interferometry, cosmic microwave background, cosmology

1. INTRODUCTION

The angular power spectrum of the CMB contains information on the structure in the Universe that existed at the epoch of decoupling at $z \sim 1000$. Angular scales less than 1° are particularly interesting, as many cosmological models predict acoustic peaks in the angular power spectrum at sub-degree scales, the amplitude and position of which are highly sensitive to cosmological parameters. Within the context of a given theory, cosmological parameters such as the Hubble Constant, H_0, and the mass density of the Universe, $\Omega_0 \equiv \rho/\rho_{crit}$, can be estimated from observations of CMB anisotropy. Although there have been many CMB experiments conducted in recent years which have detected a significant increase in power at degree and sub-degree scales, none has yielded a definitive confirmation of acoustic peaks in the CMB anisotropy.

The DASI experiment, a thirteen element interferometer being built by the Center for Astrophysical Research in Antarctica (CARA, a NSF Science and Technology Center) at the University of Chicago, will provide high signal-to-noise images of CMB anisotropy and sample the CMB power spectrum in the range $\ell = 160 - 710$ with $\Delta\ell \sim 30$ (see Figure 1). Together, DASI and the Cosmic Background Imager (CBI) currently under development at Caltech, will allow the CMB angular power spectrum to be measured continuously from $4'$ to 1.15°, covering the first acoustic peak through the damping tail in the standard Cold Dark Matter (CDM) model.

Interferometers have several features which make them an attractive choice for high sensitivity imaging of CMB anisotropy. An interferometer measures the Fourier transform of the sky signal, determining directly its angular power spectrum with well-defined window functions. In contrast to swept or chopped beam experiments with filled apertures, an interferometer may be used to produce two dimensional images of the sky in a straightforward manner; an interferometer is not limited to differencing the sky signal only along constant elevation scans. Rapid phase-switching schemes (> 10 kHz) can be used to effectively eliminate instrumental offsets.

While the stability of interferometry and its natural rejection of unwanted noise is well appreciated, many of these desirable properties arise from the clear and fairly large separation between the individual elements of the interferometer. Their beams typically trace completely independent paths through the atmosphere and do not overlap significantly until beyond the troposphere (i.e., the far field of the interferometer). Furthermore the resulting differential Doppler shift of the individually mounted elements toward the source of interest (the fringe rate) provides an added level of rejection of sources of interference. For DASI, however, the far field of the entire array is only 100 m and it is much less for the shortest baselines. The fringe rates, which would be extremely small in any case,

[a] Also affiliated with: Applied Physics Department, California Institute of Technology, Pasadena, CA 91125

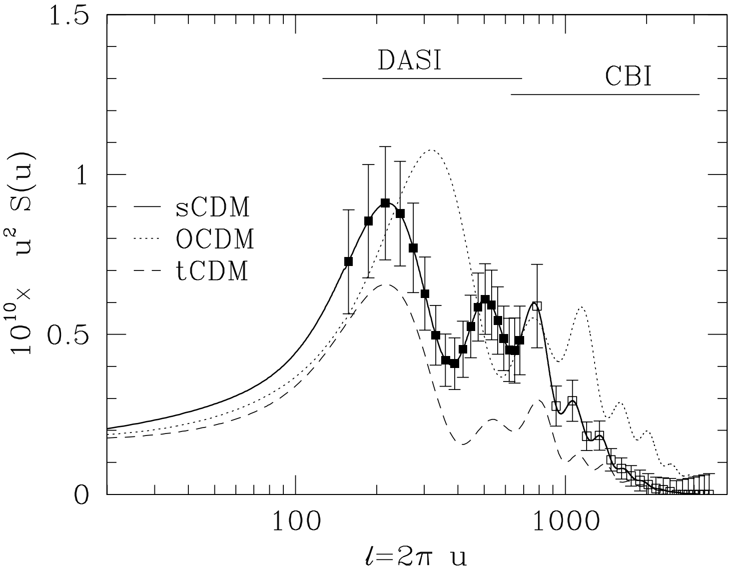

Figure 1. A plot of the expected sensitivity of DASI in six months at the Pole, and covering 1000 deg^2. The dark line is the prediction of the standard CDM model. From the Pole we should be able to image one quarter (π steradians) of the entire sky. Also shown is the expected sensitivity of the CBI for a comparable time (see Ref. 1).

are set to zero by using a common mount for all the array elements. While this simplifies the design considerably, additional attention must be paid to shielding the array from sources of interference.

This paper reviews the design of DASI. Special attention is given to the unique aspects of the design that are required to meet the challenges of imaging large scale CMB anisotropy.

2. ARRAY CONFIGURATION

The design of the array configuration was optimized to provide continuous coverage from the minimum to maximum baseline. The minimum baseline of 25 λ (25 cm), which sets the maximum angular scale, was chosen to provide coverage of the first acoustic peak in the CMB power spectrum. The maximum baseline 115 λ was chosen to overlap with the largest angular scales of the CBI.

The array elements are mounted on a single mount to allow an extremely compact configuration. To improve the u, v coverage and to provide redundancy checks, the entire array can be rotated along the line of sight. Note, the common mount prevents using standard Earth rotational synthesis techniques.

Rotational symmetry of the array configuration increases the redundancy of the array configuration under rotations along the line of sight. We chose a threefold symmetry to provide redundant baseline measurement every 60 degrees. Although the the array pattern repeats only under 120 degree rotations, the same Fourier components of the sky are measured under reflection of the array, since the sky is real and its transform Hermitian.

The array configuration resulting from the above considerations is shown in Fig. 2. Also shown is the beam pattern obtained with natural weighting of the u, v data.

3. OPTICS

Lensed corrugated horns were chosen as the antenna elements for DASI because of their compactness and low crosstalk characteristics. Each horn has a 20 cm diameter, as large as possible within the constraint of minimum baseline length, in order to achieve maximum sensitivity and to increase the u, v plane coverage for efficient mosaicing. The full width half power (FWHP) angle of the main beam is 3.4°. Corrugated horns have the advantage of an

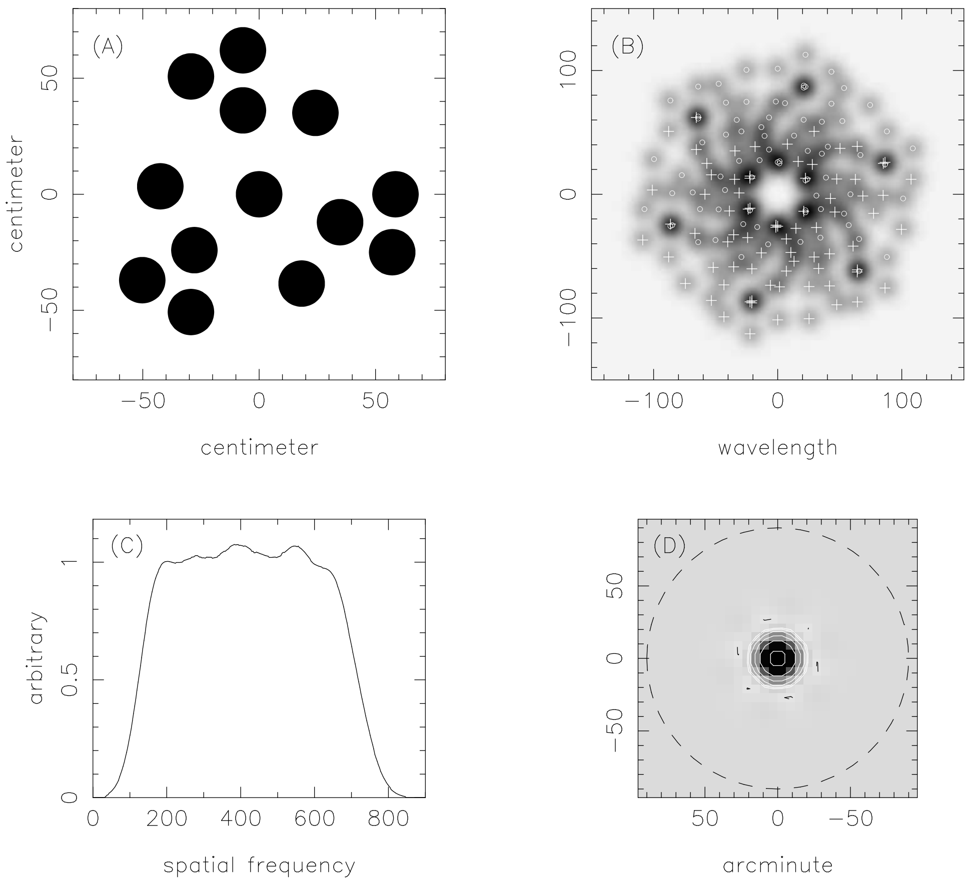

Figure 2. A configuration for the DASI elements. A) The threefold symmetric feed horn arrangement. B) The resulting instantaneous u, v coverage is shown by the points. The u, v data at each point is convolved with the autocorrelation of the aperture illumination; this weighting is shown by the grayscale. C) The azimuthal average of the u, v coverage shown in panel B. The spatial frequency is shown as a function of the index l of the spherical harmonic expansion ($l \approx 2\pi$u). Using mosaicing techniques, one can resolve spectral features over this range with a resolution set by the number of fields imaged. D) The resulting synthesized beam. The contour levels are $\pm 2.5, 5, 10, 20, 40$, and 80% of the peak. The dashed circle delineates the half power response of the primary field of view.

unobstructed and tapered aperture amplitude distribution with correspondingly low sidelobes, low spillover, and minimal crosstalk between elements. A diffraction limited compact horn is achieved by combining a wide-angle (30° semi-flare angle) corrugated horn with a High Density Polyethylene (HDPE) lens to collimate the phase front at the aperture. Figure 3 depicts an exploded view of the horn/lens assembly.

The lens is meniscus with a refracting hyperbolic front surface, and a non-refracting spherical rear surface to match the spherical wavefront of the wide-angle horn.[2] This particular lens type was chosen to increase the aperture efficiency by redistributing power towards the outside of the lens. The theoretical aperture efficiency for the DASI lensed horn is 84%, compared to 69% for an unlensed diffraction limited corrugated horn. The lens material HDPE was chosen for its desirable index of refraction, low loss tangent, and machinability. With a loss tangent $\tan\delta \simeq 170$ μrad, a lens at ambient (polar) temperature contributes 2.5 K to the system noise temperature. The lens has grooves $\sim \lambda/4$ deep that act as an anti-reflection coating.

Special consideration must be given in the design of the throat section, where the mode conversion and transition to the wide flare angle occur, not to excite spurious higher order modes which would degrade the beam.[3] A throat section similar to that described in Refs. 4,5 is employed, with an extremely narrow initial groove width (0.043 cm) gradually tapering in width and depth to reduce return loss. This type of design is particularly critical when

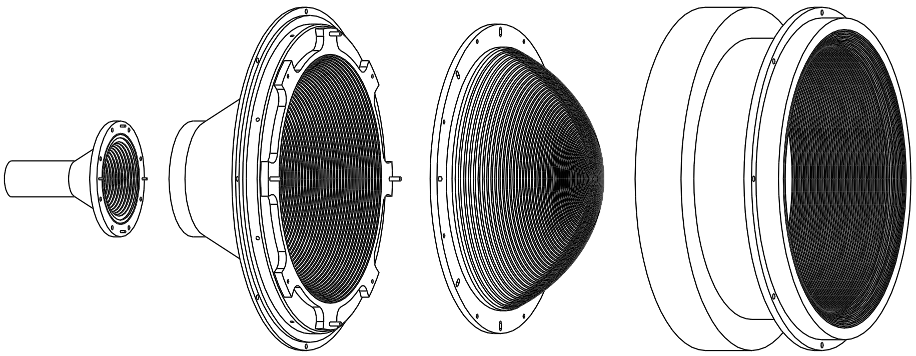

Figure 3. An exploded view of the corrugated horn, lens, and shroud. A collimating lens is combined with a wide-angle (30° semi-flare angle) flare section to produce a 20 cm diameter aperture with a diffraction limited beam pattern. The throat section, which has extremely narrow initial grooves, is electroformed separately. A high density polyethylene (HDPE) meniscus lens with a single refracting hyperbolic front surface was chosen in order to increase the aperture efficiency over that of an unlensed diffraction limited horn of equal aperture area. A corrugated shroud reduces crosstalk between antennas.

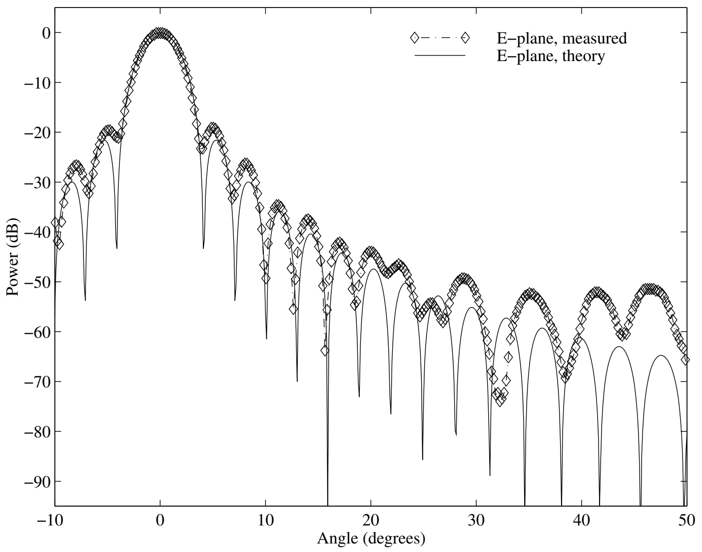

Figure 4. The measured and predicted beam pattern of the 20-cm diameter horn with lens. Theory and measurement agree well over the main beam. The lens was designed for 10K operation, but was tested at room temperature, which may account for the discrepancies between theory and measurement in the sidelobes near boresight.

combined with a wide-angle flare section to improve the impedance match to the rapidly increasing inner diameter of the horn. The measured return loss is $<$ -27 dB across the band without the lens, and $<$ -20 dB with lens. The predicted and measured beam pattern of the lensed horn is shown in Figure 4.

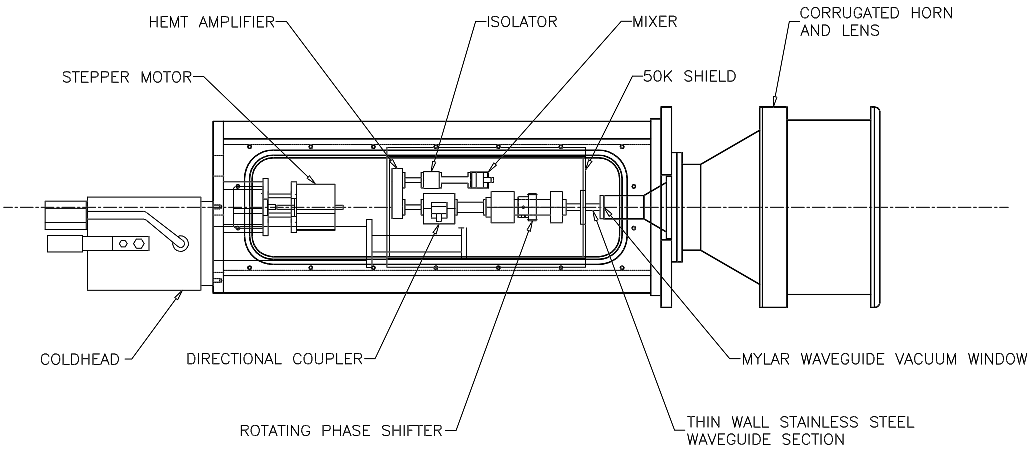

Figure 5. Cut away of a receiver. The major components are labeled.

4. RECEIVERS

The Ka–band, 26 – 36 GHz, was chosen for the availability of low-noise HEMT amplifiers,[6,7] for optimum atmospheric transmission and stability, and for low contamination from foreground emission. Dust emission is negligible at wavelengths exceeding several mm. Nonthermal emission from radio point sources, however, can be considerable. These sources will be identified and monitored using an external facility, such as the Australian array (ACTA).

A cut away view of the receiver is shown in Figure 5. The corrugated horn, lens, and shroud are discussed in the section 3. The thermal break is made by a thin wall stainless steel waveguide between the feed horn and the polarizer. The vacuum seal is made at the interface between the stainless waveguide and the throat section of the horn.

The receivers are very similar to those used to measure the Sunyaev Zel'dovich effect at 1-cm on the OVRO and BIMA arrays.[8] Based on the performance of these receivers with four stage InP HEMT amplifiers, we expect receiver noise temperatures of 12 K to 16 K, including the contribution from the warm lens.

The receivers are sensitive to only one polarization. To reduce the sensitivity to linearly polarized foreground emission, such as synchrotron emission, we utilize 1/4 wave polarizer to transform form the linear polarization of the amplifier to circular polarization.

The polarizer also serves to reduce cross talk between array elements. By adding a rotating 1/2 wave polarizer between the 1/4 wave polarizer and the feed, we modulate the phase of any noise wave emitted from one receiver and received by another, for example the out–going noise wave from the first stage amplifier. By modulating all array elements synchronously we reduce the amount of cross talk without affecting the phase of astronomical signals.

The front plate of the receiver is used to attach the receivers to the telescope. The relative pointing of the array elements is controlled to within ten arcseconds by ensuring the feed patterns are orthogonal to this precision ground front plate.

5. CORRELATOR

The DASI correlator system is essentially identical to that designed at Caltech for the CBI project. The 2-12 GHz IF signals from each of the 13 receiver local oscilators are mixed down into 10 1 GHz wide bands. Ten identical correlators then compute the complex correlation of all baselines in each of the 1-2 GHz bands. The bandwidth of 1

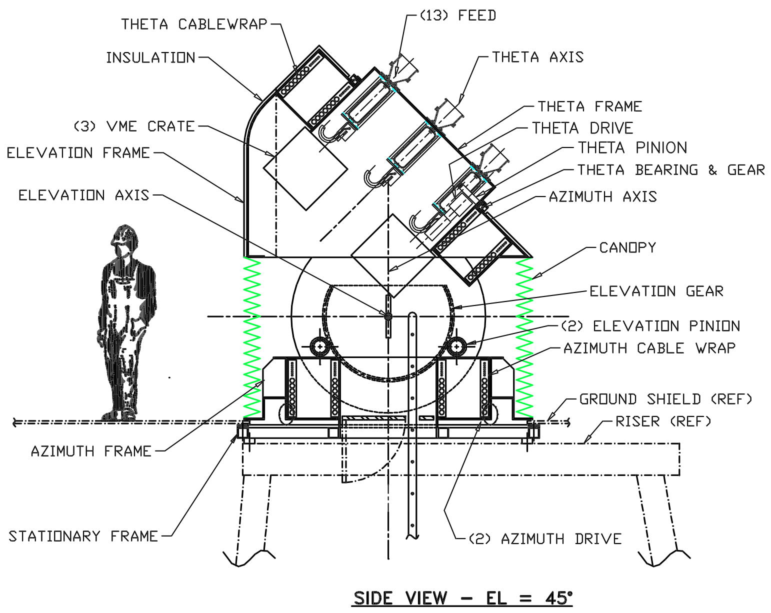

Figure 6. Cut away of the DASI telescope. A temperature controlled cabin within the telescope structure is accessed via a ladder from a room below.

GHz is a compromise between spectral resolution, necessary for characterization and removal of foreground sources, and cost of the correlator. In each 1 GHz band, an array of Gilbert cell multipliers produces the complex correlations for each of the 78 baselines. The output of the multipliers are integrated for 25.6 μs and then digitized. The phases of the 13 receiver local oscillators are modulated with shifts of 180° causing the sign of the correlation to reverse between integration periods. The digitized signals are added into an accumulator with a sign corresponding to the phase state of the LOs for each baseline. After a sequence of 32 integration periods, the accumulated signals have no DC offset and are insensitive to low frequency noise. The results of the accumulator can be be read out on time scales from .82 ms to .84 s.

A prototype unit has been measured to have an efficiency of $> 95\%$. The quadrature channels have been measured to have phase errors of less than 3 degrees. Each receiver local oscillator has a 90° phase switch which allows the characterization of these small quadrature errors. Each of the 10 1 GHz correlator modules is built onto a single 9U $\times$ 340 mm VME card. The compact size of the correlator allows it to be rigidly attached to the back of the aperture rotation axis of the telescope. Thus, instabilities associated with the flexing of cables carrying RF signals are eliminated. The response of the correlator is calibrated by injecting a stable wide-band correlated signal into the input of each of the receivers. This allows the instrument to be accurately calibrated in the time between absolute calibrations with planets.

6. MOUNT

The mount for DASI must meet stringent pointing and tracking criteria, and be able to weather the extreme environmental conditions at the South Pole. In order to be able to accurately subtract point sources and mosaic multiple fields, the pointing error must be less than a few degrees of the narrowest fringe spacing on the sky. This corresponds to a very stringent pointing requirement of 5 arc-seconds in azimuth and elevation. Additionally, the aperture plane is able to rotate about its central axis, both to improve the synthesized beam through rotational synthesis, and to provide for consistency checks and offset subtraction by exploiting the 3-fold rotational symmetry of the aperture array pattern. The mount must be operable in the extreme cold conditions at the South Pole, where the temperature averages -30 C in the Austral summer, and -60 C in the Austral winter.

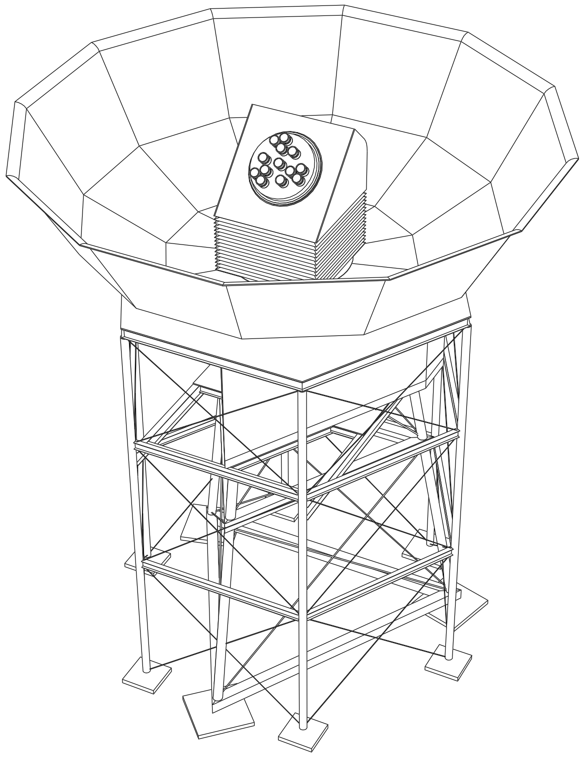

Figure 7. DASI mounted on the 11 m high tower. The tower is connected to the Martin A. Pomerantz Observatory (MAPO) building (not shown). Access is enabled by a room under the telescope connected directly to the laboratory building.

The mount is being designed in collaboration with TIW Systems, Inc..[9] As shown in Figure 6, it consists of a counterbalanced gear and pinion elevation drive, a geared radial bearing for the aperture rotation axis, and a 4 wheel azimuth drive, with matching symmetry on the azimuth ring supports for homologous deformation of the ring. The azimuth and elevation axes have 2 drive motors each with differential torque to eliminate backlash. The telescope is well insulated, with a flexible insulated sleeve between the elevation and azimuth structures to maintain a comfortable working environment. In addition, the back-end electronics are temperature regulated with water cooled VME crates.

7. GROUND SHIELDS

Reflective angled ground shields are necessary to prevent the sidelobes of the interferometer from seeing correlated thermal noise from the ground and structures surrounding the instrument. The shields for DASI are shown in Figure 7. The horizon is obscured for every element of the array at all angles greater than the minimum observing angle of 25°. The geometry of the ground shields is designed to reflect the beam of each of the antennas to the cold 6 K sky for all angles off boresight $\leq 90°$. Several of the ground shield panels are hinged and may be lowered to the horizon to allow observations of planets (always at low elevation at the South Pole), and calibration with a fixed ground transmitter.

8. THE POLAR SITE

Of primary concern for the DASI site is the level and stability of the atmospheric emission. Most high dry sites have excellent atmospheric transmission at 30 GHz. Atmospheric stability, especially on angular scales of order one degree, is a more stringent requirement for CMB observations.

The high altitude (2800 m) plateau at the South Pole is an exceptional site. The low atmospheric opacity and smooth continuous airflow are ideal conditions for large field imaging. Long periods of excellent transparency and low sky noise have been used to great advantage in past years by a number of different experiments (see, for example, Refs. 10–13). Atmospheric analysis of the 1996 - 1997 Austral summer Python experiment 40 GHz swept beam data indicates that the atmosphere is bimodal in nature with very good stability ~75% of the time, during which the experiment is instrument noise limited.[14] The South Pole has negligible diurnal fluctuations; in addition the Sun is absent for 6 months of the year and is easily shielded during the Austral summer. From the South Pole, the largest dark region from the IRAS Sky Survey is accessible, and the DASI fields will overlap with those of Antarctic long duration balloon experiments as well as previously observed fields.

ACKNOWLEDGMENTS

We thank the entire CBI team for their help with this project, Marian Pospielsalski and NRAO for assistance with the HEMT amplifiers, and CARA and the University of Chicago for generous support. JEC acknowledges a NSF Young Investigator award and a David and Lucile Packard Foundation Fellowship. DASI is a project of CARA, a NSF Science and Technology Center, which is funded through grant number OPP-8920223.

REFERENCES

1. M. White, J. E. Carlstrom, and M. Dragovan, "Interferometric observation of cosmic microwave background observations," *ApJ submitted* , 1998.
2. P. J. B. Clarricoats and P. K. Saha, "Radiation pattern of a lens-corrected conical scalar horn," *Elecron. Lett.* **21**, pp. 592–593, 1969.
3. B. M. Thomas, G. L. James, and K. J. Greene, "Design of wide-band corrugated conical horns for cassegrain antennas," *IEEE Trans. Antennas and Propagation* **34**(6), pp. 750–757, 1986.
4. X. Zhang, "Design of conical corrugated feed horns for wide-band high-frequency applications," *IEEE Trans. Microwave Theory and Techniques* **41**(8), pp. 1263–1274, 1993.
5. P. F. Goldsmith, "Quasi-optical techniques at millimeter and submillimeter wavelengths," in *Infrared and Millimeter Waves*, vol. 6, pp. 277–343, Academic, (New York), 1982.
6. M. W. Pospieszalski, "Ultra–low–noise receivers for the 1 to 120 GHz frequency range," in *Proc. of 23rd European Microwave Conf*, vol. 6, pp. 73–79, 1993.
7. M. W. Pospieszalski, L. Nguyen, M. Lui, T. Lui, M. Thompson, and M. J. Delaney, "Very low noise and low power operation of cryogenic AlInAs/GaInAs/InP HFET's," in *Proc. 1994 IEEE MTT-S Int. Microwave Symp.*, pp. 1345–1346, 1994.
8. J. E. Carlstrom, M. Joy, and L. Grego, "Interferometric imaging of the Sunyaev–Zeldovich effect at 30 GHz," *ApJ* **456**, pp. L75–L78, 1996.
9. TIW Systems, Inc., 2211 Lawson Lane, Santa Clara, CA 95054.
10. G. S. Tucker, G. S. Griffin, H. T. Nguyen, and J. B. Peterson, "A search for small-scale anisotropy in the cosmic microwave background," *ApJ* **419**, pp. L45–L48, 1993.
11. M. Dragovan, J. Ruhl, G. Novak, S. Platt, B. Crone, R. Pernic, and J. Peterson, "Anisotropy in the microwave sky at intermediate angular scales," *ApJ* **427**, pp. L67–L70, 1994.
12. J. O. Gundersen, M. Lim, J. Staren, C. A. Wuensche, and N. Figueiredo et al., "Degree-scale anisotropy in the cosmic microwave background: SP94 results," **443**, pp. L57–L60, 1995.
13. S. R. Platt, J. Kovac, M. Dragovan, J. B. Peterson, and J. E. Ruhl, "Anisotropy in the microwave sky at 90 GHz: Results from Python III," *ApJ* **475**, pp. L1–L4, 1997.
14. O. P. Lay et al. 1998 in preparation.